COMPARISON OF SHEARED ROTATION EFFECTS ON KINETIC STABILITY IN TOKAMAK PLASMAS

G. Rewoldt, M. S. Chance, T. S. Hahm, and W. M. Tang

Plasma Physics Laboratory, Princeton University
Princeton, New Jersey 08543-0451

Sheared rotation dynamics are widely believed to have significant influence on experimentally observed confinement transitions in advanced operating modes in major tokamak experiments, for example in those which can have reversed magnetic shear regions in the plasma interior. The high-n toroidal drift modes destabilized by the combined effects of ion temperature gradients and trapped particles in toroidal geometry can be strongly affected by radially-sheared $\mathbf{E} \times \mathbf{B}$ plasma rotation. In previous work with the FULL comprehensive linear microinstability code[1], a simplified rotation model[2] including only toroidal rotation was employed to help assess the associated impact on confinement. A more complete rotation model, that allows general flux-coordinate toroidal geometry, has been developed which now includes contributions to the total radial electric field from toroidal and poloidal rotation and from the ion pressure gradient. Applying this more complete model to enhanced reversed shear cases for TFTR produces results on the role of rotation that are consistent with the well-known heuristic criterion for complete stabilization, $i.e.$, the criterion that the $\mathbf{E} \times \mathbf{B}$ rotation shearing frequency[3] be greater than the linear growth rate without rotation. When the calculation is performed using data from new experimental measurements of the poloidal velocity[4], significantly stronger stabilization is found than when neoclassical estimates of the poloidal velocity are employed.

The implementation of this new (E_r) rotation model in the FULL code with the ballooning representation was described in some detail in Ref. [5], and results were presented there for several TFTR cases in comparison with the old (V_ϕ or Artun) model. It was shown in Refs. [6] and [7] that the ballooning representation breaks down for substantial values of the Mach number. However, it was also shown in Ref. [6] that this representation is still usable for small values of the Mach number, and we will thus continue to employ it here. A prescription for the ballooning parameter θ_0 is needed, in addition to the rotation model itself. The simplest choice, $\theta_0 = 0$, which is the usual choice in the absence of rotation, was employed in Ref. [5]. An alternative would be to average the eigenfrequency over $0 \leq \theta_0 \leq 2\pi$, as specified in Ref. [7]. However, a better prescription can be determined as follows: One-dimensional (ballooning representation) and two-dimensional calculations for toroidal drift modes have been compared for the old rotation model in Ref. [8], and a way of modeling one of the missing two-dimensional effects in the one-dimensional calculation was found there. This was the effect of 'eigenfunction shearing', in which the individual eddies in the two-dimensional eigenfunction twist as the Mach number increases, and the value of k_r at $\theta = 0$ increases. θ_0 (which enters the ballooning

representation expression for k_r) will have an 'average' or 'effective' value which in general is nonzero, except in the case of zero rotation. By making this 'effective' value of θ_0 an explicit, fitted function of the local Mach number M, reasonable quantitative agreement was obtained for the growth rates between the one-dimensional and two-dimensional calculations; the fitted form of the ballooning parameter obtained in Ref. [8] was $\theta_0(M) = -6.83M/[M^2+(0.02)^2]^{1/4}$. This is a way of putting one of the otherwise missing two-dimensional effects into a one-dimensional, ballooning formalism calculation. It should be emphasized that this eigenfunction shearing form of $\theta_0(M)$ is not part of the E_r rotation model, but is added on from modeling of results, whereas all of the E_r rotation model itself comes from the derivations of Ref. [5]. This form will be employed here in the FULL code along with the new E_r rotation model, in comparison with $\theta_0 = 0$.

To investigate the effects of rotation, we start with a case that was investigated in Ref. [8] using the old "V_ϕ" rotation model, and recalculate the linear growth rates γ using our new E_r rotation model. This is a case with experimentally-derived density and temperature profiles and a numerically-calculated MHD equilibrium for the TFTR "enhanced reversed shear" (ERS) discharge 84011, at $t = 2.70$ s, just before the ERS confinement transition time. We do the calculation for the electrostatic toroidal drift mode, including a carbon impurity species and a hot beam species with a slowing-down equilibrium distribution function. For this case we will use the E_r profile obtained from the radial force balance relation $E_r = V_\phi B_\theta - V_\theta B_\phi + (1/e_C n_C) dp_C/dr$, with all the quantities on the right hand side being experimentally determined, except that for V_θ we use $V_\theta^{\rm neo}$, the neoclassical estimate for V_θ. We define the local Mach number $M \equiv |v_E|/v_i$, with $v_E \equiv c\mathbf{E} \times \mathbf{B}/B^2$, and we vary M artificially by multiplying the entire E_r profile by a constant, and we multiply the V_ϕ profile by the same constant. Results for γ versus M for this TFTR ERS case are shown in Fig. 1a. One curve shows the results for the E_r model with $\theta_0 = 0$, while the other adds the additional eigenfunction shearing effect through $\theta_0(M)$, and this is seen to give a moderate additional stabilizing effect for this case.

Another TFTR ERS case of interest is for discharge 103794, at $t = 2.0$ s. We compare three different sets of input data for the E_r radial profile: $E_r = 0$, corresponding to an absence of rotation, $E_r = E_r(V_\theta^{\rm neo})$, where the neoclassical estimate of V_θ is used to calculate E_r from the radial force balance relation, and $E_r = E_r(V_\theta^{\rm meas})$, where the spectroscopically measured profile[4] of V_θ is used instead. The radial profiles for $V_\theta^{\rm neo}$ and $V_\theta^{\rm meas}$ can be substantially different, by an order of magnitude or more, at localized times and places in the discharge. Correspondingly, the associated profiles for E_r, shown in Fig. 3 of Ref. [5], are drastically different in the inner half of the cross-section. The results for the linear growth rates of the electrostatic toroidal drift mode are shown in Fig. 1b for the three choices for E_r. For $r/a > 0.3$, the growth rate profiles are almost identical for $E_r = 0$ and for $E_r(V_\theta^{\rm neo})$, while the growth rate profile for $E_r(V_\theta^{\rm meas})$ is somewhat narrowed and is lowered by $\sim 30\%$, all for $\theta_0 = 0$. The results for $E_r = E_r(V_\theta^{\rm meas})$ with $\theta_0 = \theta_0(M)$ are also shown in Fig. 1b. The additional

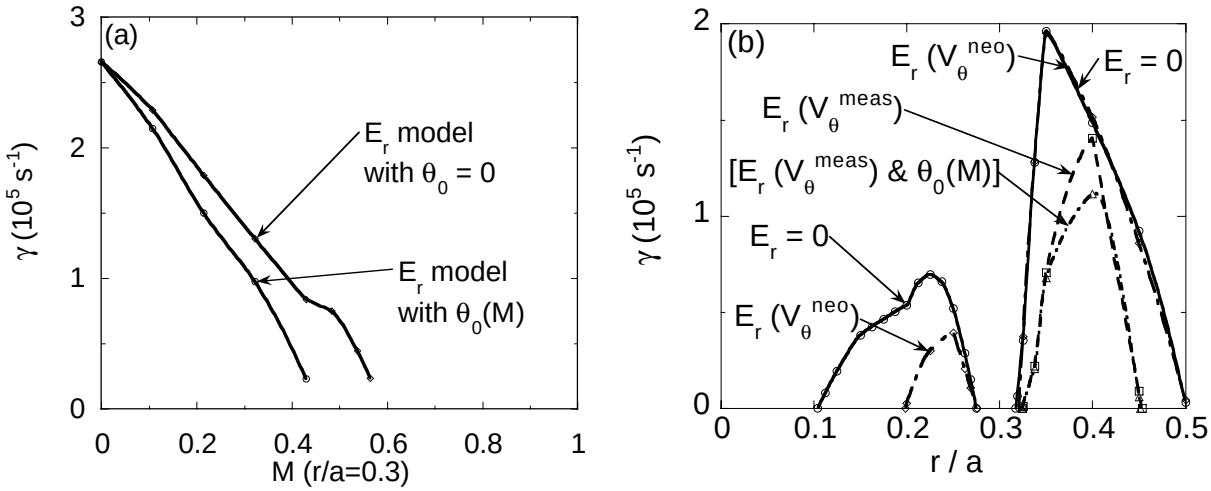

Figure 1. (a) Linear growth rate γ versus M for TFTR ERS discharge 84011 at $t = 2.70$ s, for $r/a = 0.300$, $n = 41$, $k_\theta \rho_i = 0.79$, and $V_\phi \propto M$. (b) Radial profile for γ for TFTR ERS discharge 103794 at $t = 2.0$ s for $k_\theta \rho_i = 0.81$, with $E_r = 0$, $E_r(V_\theta^{\rm neo})$, and $E_r(V_\theta^{\rm meas})$, all with $\theta_0 = 0$, and for $E_r(V_\theta^{\rm meas})$ with $\theta_0 = \theta_0(M)$.

'eigenfunction shearing effect' decreases the maximum growth rate only moderately, and the radial marginal points where $\gamma = 0$ are moved almost not at all.

Combining previous results for our new E_r rotation model of Ref. [5] with the 'eigenfunction shearing' model of Ref. [8], we have shown that including the two-dimensional 'eigenfunction shearing' effect in a one-dimensional, ballooning representation calculation changes the results only moderately, at least for the TFTR cases considered here. In future work, other cases for other major tokamaks such as DIII-D, JET, JT-60U, NSTX, and C-MOD will be considered with this improved linear rotation model and the eigenfunction shearing model, as well as additional TFTR cases, and the results will be compared.

Acknowledgements. Work supported by U.S. Department of Energy Contract DE-AC02-76-CHO-3073.

References

[1] G. Rewoldt, W.M. Tang and M.S. Chance: Phys. Fluids **25**, 480 (1982); G. Rewoldt, W.M. Tang and R.J. Hastie: Phys. Fluids **30**, 807 (1987).

[2] M. Artun, Ph.D. Dissertation, Princeton University, 1994; M. Artun, W.M. Tang and G. Rewoldt: Phys. Plasmas **2**, 3384 (1995).

[3] T.S. Hahm and K.H. Burrell: Phys. Plasmas **2**, 1648 (1995).

[4] R.E. Bell: Bull. Am. Phys. Soc. **42**, 1945 (1997).

[5] G. Rewoldt, M.A. Beer, M.S. Chance, T.S. Hahm, Z. Lin and W.M. Tang: Phys. Plasmas **5**, 1815 (1998); *More algebraic detail is given in:* G. Rewoldt, M.A. Beer, M.S. Chance, T.S. Hahm, Z. Lin and W.M. Tang: Princeton University, Plasma Physics Laboratory Report PPPL-3276 (1997), *available in pdf and postscript formats at* http://www.pppl.gov/.

[6] F.L. Waelbroeck and L. Chen: Phys. Fluids B **3**, 601 (1991).

[7] J.B. Taylor, H.R. Wilson, and J.W. Connor: Plasma Phys. Controlled Fusion **38**, 243 (1996).

[8] G. Rewoldt, L.L. Lao and W.M. Tang: Phys. Plasmas **4**, 3293 (1997).